

## QUASI-3D SIMULATION OF COMPRESSIBLE UNSTEADY FLOWS THROUGH ICE-MANIFOLDS

Gheorghiu, Victor\*

University of Applied Sciences Hamburg, Germany

**KEYWORDS** - Gas exchange processes simulation, Coupling of 1D and 3D compressible flows, Computing time saving method, Manifold design, ICE

**ABSTRACT** - The design of intake and exhaust manifolds for ICE has been an important application of unsteady fluid dynamics for many years. A first purpose of these simulations is the optimizing of the filling, the accordance with the turbocharger etc. of ICE about wide load and engine speed intervals. A second purpose is the estimating of the required initial conditions for the simulation of the in cylinder air/fuel mixture formation and burning processes, which must have knowledge about the quantity, the composition and the flow-field of the intake charge.

Since the computation costs are high for the implementation of unsteady fully three-dimensional (3D) simulations of the gas exchange processes usual one-dimensional (1D) simulations are used instead. In this case, since the 1D-simulation of the gas flow processes cannot describe the whole reality (i.e. the three-dimensionality) of the gas flow correctly, curvatures, asymmetry of the pipes, and channels in the simulation are disregarded. In order to find a compromise procedure for this situation, the **quasi-3D method** is presented, that improves the quality of the 1D-simulation results noticeably without increasing the cost of computation proportionally. This method is based on the 1D partial differential equations (PDEs), which model the unsteady compressible flow process of a viscous fluid.

The quasi-3D method is introduced now in the following steps:

1. The 3D flow equations are deduced appropriately, as to consider the distortion of the velocity distribution (size and direction) in each pipe cross-section. Their integration over the pipe cross-section results in the 1D flow equations, the terms of which still contain integrals of the velocity distribution. In the following, these integrals are designated as **adjustment coefficients** of the 1D-flow. The 1D-flow equations together with the adjustment coefficients form **the quasi-3D PDEs**.
2. The adjustment coefficients are further treated as temporally independent parameters in each pipe cross-section. For integration of the quasi-3D PDEs the total variation diminishing finite difference method (as example) is used.
3. The determination of the adjustment coefficients take place with the help of a steady 3D-simulation (here FIRE is used), which is only done for steady forward and reverse flow through the pipes. The resulted 3D flow velocity fields are appropriately processed to produce the requested adjustment coefficients.
4. The quasi-3D method can be used now for the accurate simulation of manifold flow processes throughout the full engine cycles.
5. The flow velocity CA-variations together with the adjustment coefficients enable determination of the 3D flow velocity distributions related to CA in the cylinder interfaces.

Apart from the theoretical basics, the quasi-3D method is applied to a one-cylinder research diesel engine. The comparison between simulation results and pressure measurements in multi-point intake pipe at several engine speeds and loads is shown and commented in detail.

MAIN SECTION - The purpose of this paper is to present some simulation results by means of the **quasi-3D method** of the compressible unsteady flow of a viscous fluid through pipes and manifolds of internal combustion engines (ICE). The quasi-3D method can describe the influence of the gas flow three-dimensionality correctly (i.e. curvatures, asymmetry of the pipes, channels etc.) by means of the **adjustment coefficients**. The using of the quasi-3D method improves the simulation quality noticeably (compared to the classical 1D-simulation) without increasing the cost of computation proportionally (compared to the classical unsteady 3D-simulation).

Apart from some theoretical basics about computation and choose of the adjustment coefficients sets, the quasi-3D method is applied (as an example) to a one-cylinder research diesel engine. The comparison between simulation results in intake pipe and pressure measurements in some point of the intake pipe at some engine speeds and two loads is shown and commented.

## PRESENTATION OF THE QUASI-3D PDEs AND THEIR INTEGRATION

For the theoretical development of the 1D PDEs it is helpful to use the stream thread notion. In this case, the lateral surface of the stream thread is impermeable to matter, since this area itself is formed by streamlines. The classical stream thread notion is generally characterized as follows: *The variations of all state variables in the cross direction of a stream thread are much lower than in its longitudinal direction*, (8). The quasi-3D stream thread notion supplements the classical one by accepting that the *flow velocity varies significant in the cross direction too*, (3), (4).

In case of a pipe flow, since the tube wall (similar to the stream thread lateral surface) is impermeable to matter, the quasi-3D stream thread notion can be put into practice perfectly. This notion has the advantage that one can take into account the effect of the interior curvatures, asymmetry etc. of the pipes and channels on the resulting distorted velocity field.

The 3D flow equations are deduced appropriately, as to consider the distortion of the velocity distribution (size and direction) in each quasi-3D stream thread (pipe) cross-section. Their integration over the pipe cross-section results in the 1D flow equations, the terms of which still contain integrals of the velocity distribution. These integrals are designated as **adjustment coefficients** of the 1D flow, since they describe the 3D distribution of the gas flow velocity. The 1D flow equations together with the adjustment coefficients (s. the definitions [5], [6] and [7]) form the **quasi-3D PDEs** (s. equation [1] with the vectors [2], [3] and [4]), (3), (4).

The adjustment coefficients **a**, **b** and **g** (**b** is known as *Coefficient of Boussinesq*, (1), (2)) are treated as temporally independent parameters in each pipe cross-section.

## Symbols

<b>r</b>	= gas density
<b>p</b>	= gas pressure
<b>k</b>	= gas isentropic exponent
$r_i$	= mass fraction of the gas component <i>i</i> (for ex. of the exhaust gases)
<b>A</b>	= pipe cross-section
<b>v</b>	= local flow velocity

$$\mathbf{U}_t + \mathbf{F}(\mathbf{U})_x = \mathbf{H}(\mathbf{U}) \quad [1]$$

$$\mathbf{U} = \begin{bmatrix} r \\ r \cdot C \\ \frac{p}{k-1} + g \cdot \frac{r \cdot C^2}{2} \\ r_i \cdot r \end{bmatrix} = \begin{bmatrix} U_1 \\ U_2 \\ U_3 \\ U_4 \end{bmatrix} \quad [2]$$

$c$	= local axial flow velocity
$C$	= average value of $c$ over $A$ (s. definition 8)
$a, b, g$	= adjustment coefficients
$I_D$	= wall friction coefficient
$R_G$	= gas constant (ideal gas)
$D_H$	= pipe hydraulic diameter
$k$	= heat transfer coefficient
$T$	= gas temperature
$T_W$	= pipe wall temperature
$z$	= loss coefficient

### Indices

$t, x$	= partial differentiation with respect to time $t$ or to space $x$
--------	--

$$F(\mathbf{U}) = \begin{bmatrix} U_2 \\ (k-1) \cdot U_3 + \left( b - \frac{k-1}{2} \cdot g \right) \cdot \frac{U_2^2}{U_1} \\ \frac{U_2}{U_1} \cdot \left( k \cdot U_3 + \frac{a-k \cdot g}{2} \cdot \frac{U_2^2}{U_1} \right) \\ \frac{U_2}{U_1} \cdot U_4 \end{bmatrix} \quad [3]$$

$$H(\mathbf{U}) = \begin{bmatrix} -U_1 \cdot \left( \frac{A_t}{A} + \frac{U_2}{U_1} \cdot \frac{A_x}{A} \right) \\ -U_2 \cdot \left[ \left( \frac{A_t}{A} + b \cdot \frac{U_2}{U_1} \cdot \frac{A_x}{A} \right) + \frac{1}{2} \cdot \frac{I_D}{D_H} \cdot \frac{|U_2|}{U_1} \right] \\ H_3 \\ -U_4 \cdot \left( \frac{A_t}{A} + \frac{U_2}{U_1} \cdot \frac{A_x}{A} \right) \end{bmatrix} \quad [4]$$

with

$$H_3 = \left[ - \left( \frac{A_t}{A} + k \cdot \frac{U_2}{U_1} \cdot \frac{A_x}{A} \right) - \frac{4 \cdot k}{D_H} \cdot \frac{k-1}{U_1 \cdot R_G} \right] \cdot \left( U_3 - \frac{g}{2} \cdot \frac{U_2^2}{U_1} \right) - \frac{1}{2} \cdot \frac{U_2^2}{U_1} \cdot \left[ \left( g \cdot \frac{A_t}{A} + a \cdot \frac{U_2}{U_1} \cdot \frac{A_x}{A} \right) - \frac{I_D}{D_H} \cdot \frac{|U_2|}{U_1} \right] + \frac{4 \cdot k}{D_H} \cdot T_W$$

$$a = \frac{1}{|C|^3 \cdot A} \cdot \int_{A(t)} v^2 \cdot |c| \cdot dA \quad [5]$$

$$b = \frac{1}{C \cdot |C| \cdot A} \cdot \int_{A(t)} c \cdot |c| \cdot dA \quad [6]$$

$$g = \frac{1}{C^2 \cdot A} \cdot \int_{A(t)} v^2 \cdot dA \quad [7]$$

$$C = \frac{1}{A} \cdot \int_{A(t)} c \cdot dA \quad [8]$$

### Integration of the Quasi-3D PDEs

For the integration of the quasi-3D PDEs (as example) the finite-difference method with the so-called total variation diminishing (TVD) method, Lax-Friedrichs non-MUSCL (monotonic upstream schemes approach) for the homogeneous PDEs (i.e. without source terms) is used. In order to consider the effect of the source terms from the vector  $\mathbf{H}$ , the TVD technique is integrated in a predictor-corrector procedure (7), (3), (4).

### PRESENTATION OF THE SIMULATION RESULTS AND THEIR COMPARISON WITH THE MEASUREMENTS

For validating of the simulation results, an AVL 520 one-cylinder research engine of the laboratory for Power Engineering, Piston, and Turbo Machines of the University of Applied Sciences Hamburg was used. The arrangement of the pipes and of all measuring points is represented in the Figure 1.

Figure 2 shows the 3D computing mesh of the intake pipe and intake port segment, i.e., between the intake silencer and the inlet valve. Figure 3 shows only the computing mesh of the intake channel with relative pressure cuts und flow velocity vectors (only in 10x10 resampling Cartesian grid) distributions in some (perpendicular to x-axis and 30 mm spaced) sections.

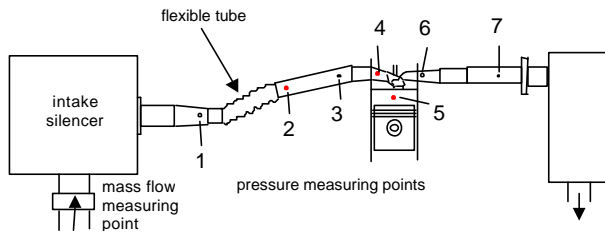


**Fig. 1** Arrangement of all measuring points

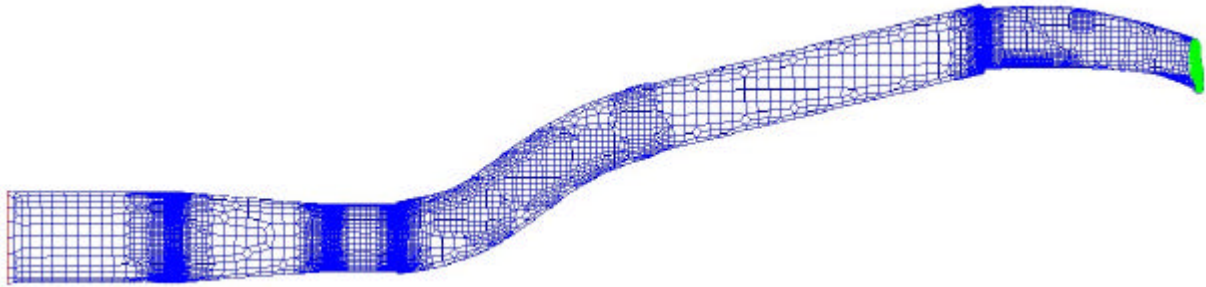


**Fig. 2** Computing mesh of the completing intake pipe

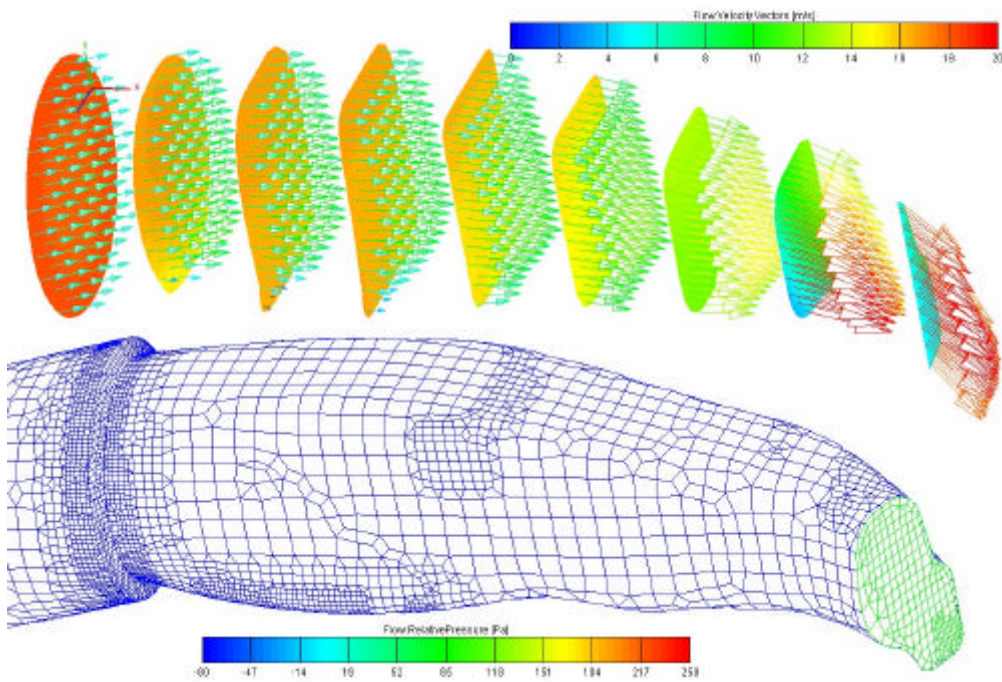


**Fig. 3** Intake channel computing mesh with relative pressure cuts and flow velocity vector distributions in some sections by 0.03 kg/s forward mass airflow

### Computing of the adjustment coefficients for STEADY forward and reverse mass flows

These simulations of the steady turbulent compressible airflow - carry out with the CFD program FIRE - are accomplished first for a compressible turbulent steady forward and reverse airflow through the intake pipe and inlet port. For computing of the adjustment coefficients **a**, **b** and **g** variations, i.e. for computing of the integrals from [5] to [8], the simulation results from FIRE are exported and with MATLAB post-processed.

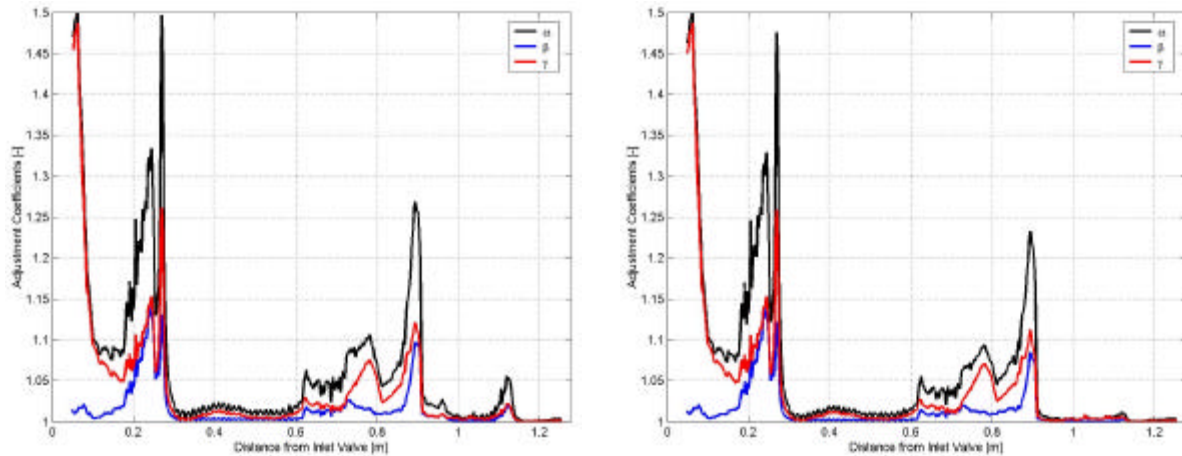


**Fig. 4** Adjustment coefficient distributions by 0.01 (left) and 0.03 kg/s forward mass airflow over the **distance from the inlet valve** (mirror representation regarding Fig. 2 and 3, i.e. the airflow is directed here from right to left)

One must test first, if the hypothesis *the height of the mass flow has now influence over the adjustment coefficients height and distribution* works. Figure 4 shows these distributions by 0.01 and 0.03 kg/s forward steady mass airflow. One remarks that the differences are negligible and consequently this hypothesis is justified.

In the case of the steady reverse flow is the situation differently. The comparison between forward (Fig. 4 right) and backward (Fig. 5 right) by 0.01 kg/s mass airflow shows practical other distribution and other height for the adjustment coefficients.

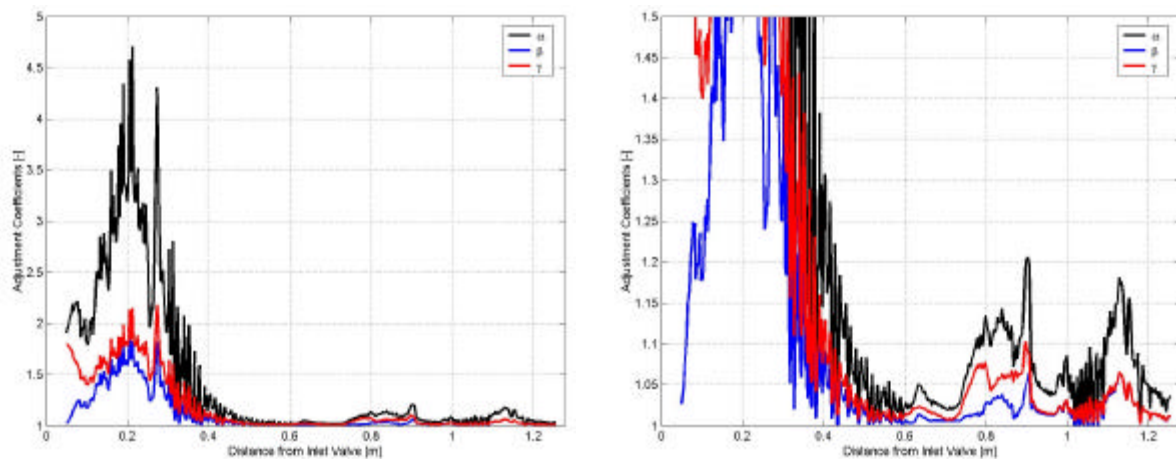


**Fig. 5** Adjustment coefficient distributions by 0.01 kg/s backward mass airflow (right with the same scale like in Fig. 4) over the **distance from the inlet valve**

### Computing of the adjustment coefficients for UNSTEADY mass flows

In this case the design example with throttle (40 mm diameter, 2 mm thickness, 45° inclination, 0.1 m away from pipe inlet (on the left side)), asymmetrical (4 mm between axes, 0.2 m away from inlet) sharp cross-section variation (from 40 mm to 30 mm diameter) and bend piece (90°, 26 mm radius, 0.26 m away from inlet) from Figure 6 is considered. In the pipe inlet remains the pressure constant and equal to the ambient pressure ( $10^5$  Pa). In the outlet is the pressure linearly varied, so that it is by 0°C (start of simulation) equal to the ambient

pressure, arises by 60°CA 60% and by 180°CA (end of simulation) 110% from the ambient pressure. That means in this example is simulated only a simplified sucking process. The selected engine speed is 5000 rpm in this case.

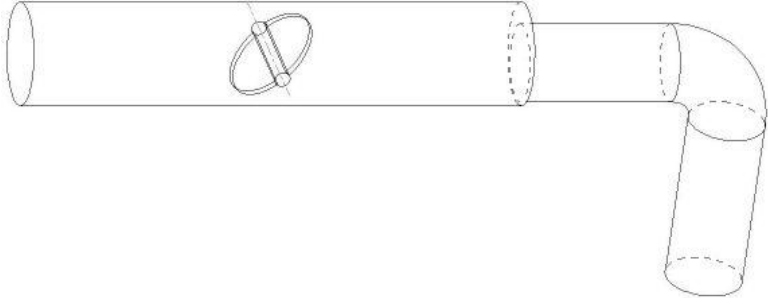


**Fig. 6** Design example of an intake pipe with throttle, sharp cross-section variation and bend piece

The results of this 3D unsteady flow simulation (as well carry out with FIRE and post-processed with MATLAB) are presented in the Figure 7 with a time-resolution of 10°CA.

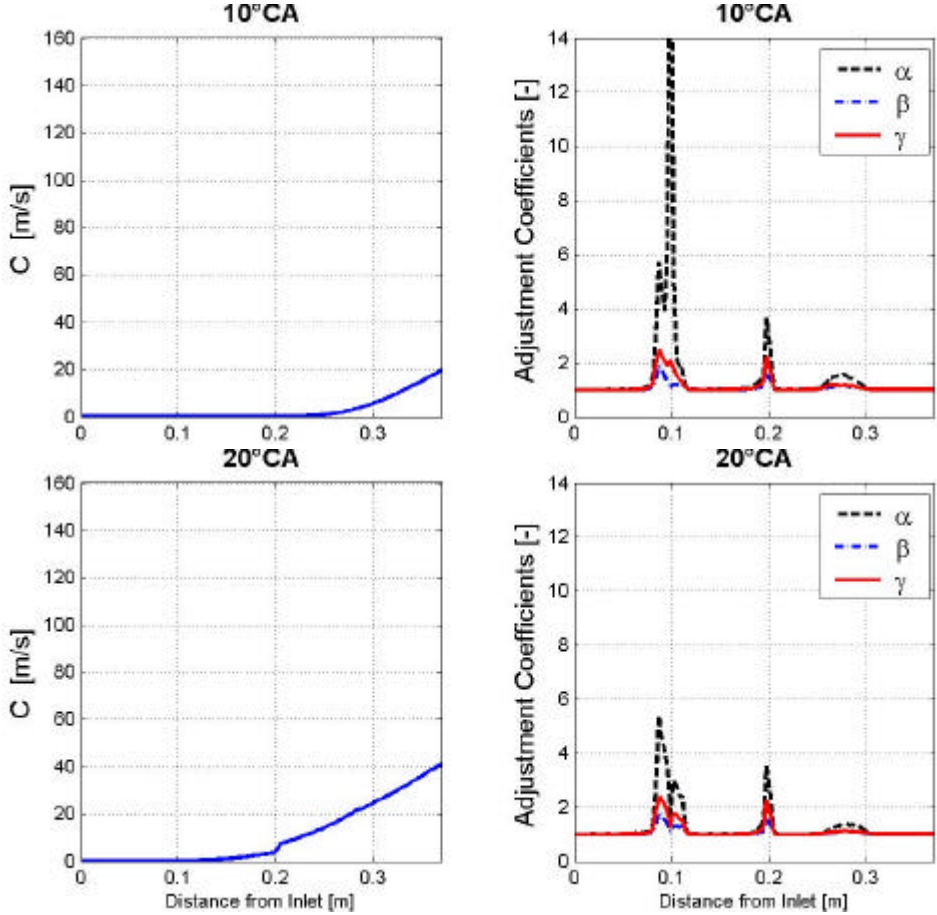


**Fig. 7** Averaged axial flow velocity  $C$  and adjustment coefficients variations

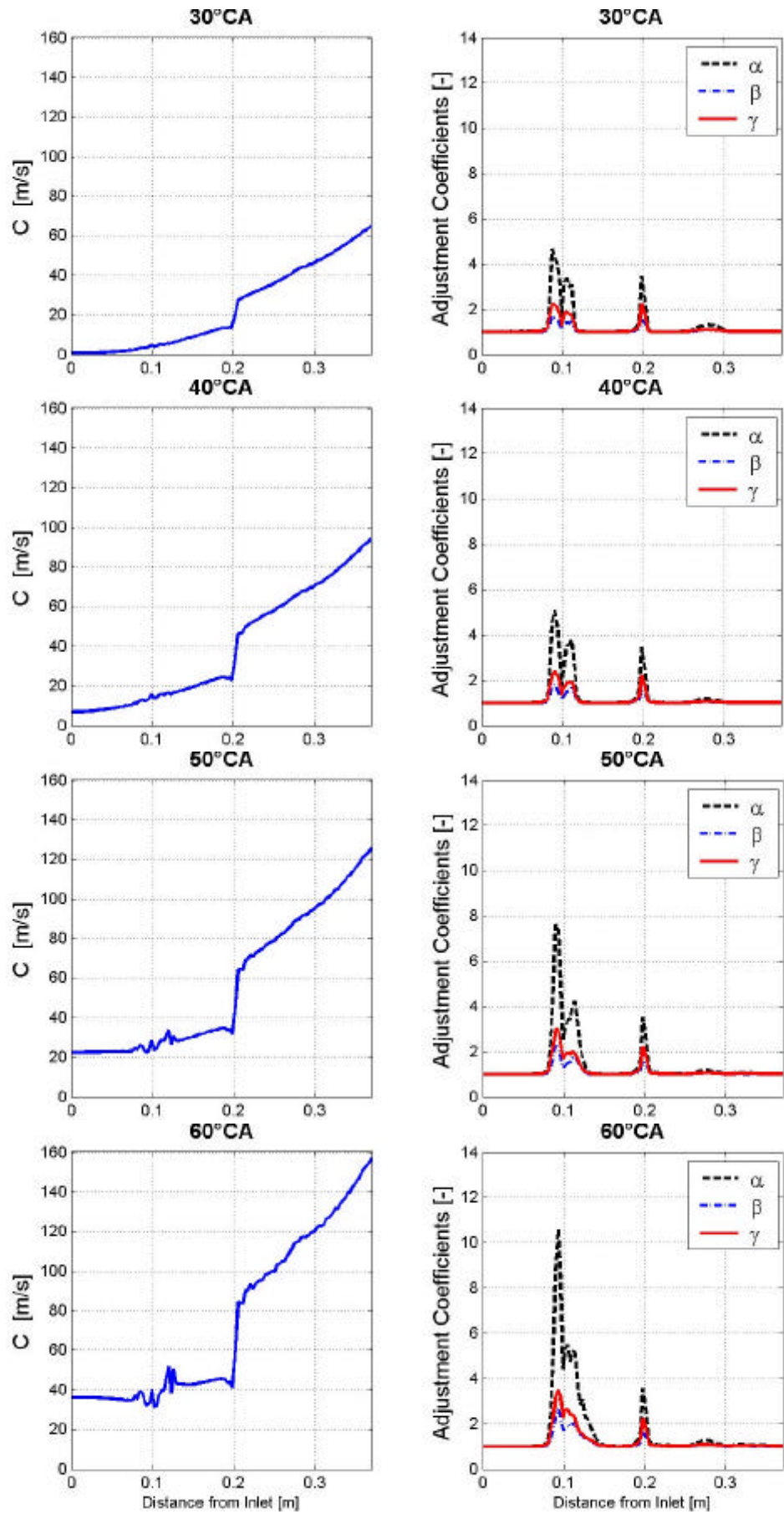


Fig. 7 Averaged axial flow velocity  $C$  and adjustment coefficients variations (continuation)

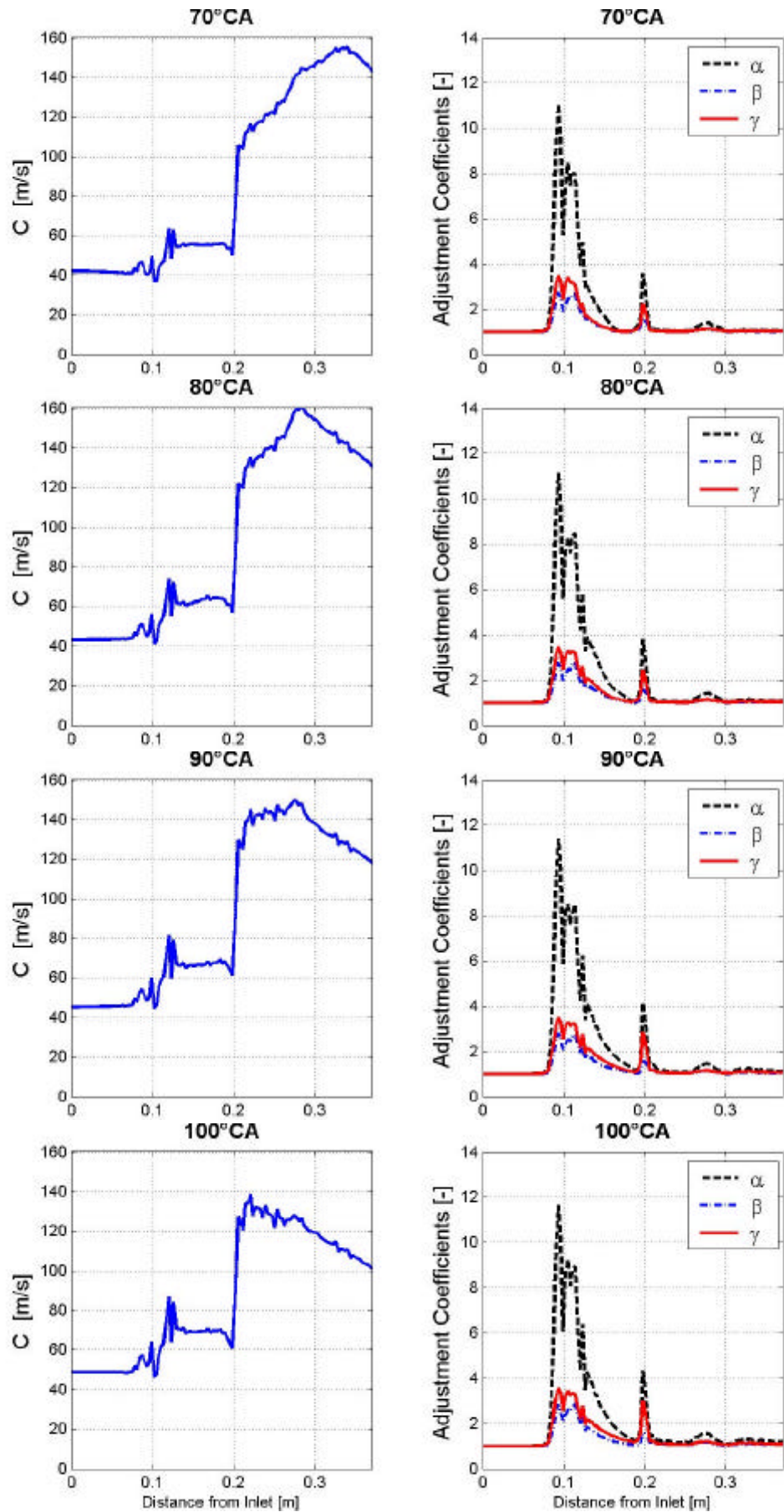


Fig. 7 Averaged axial flow velocity  $C$  and adjustment coefficients variations (continuation)

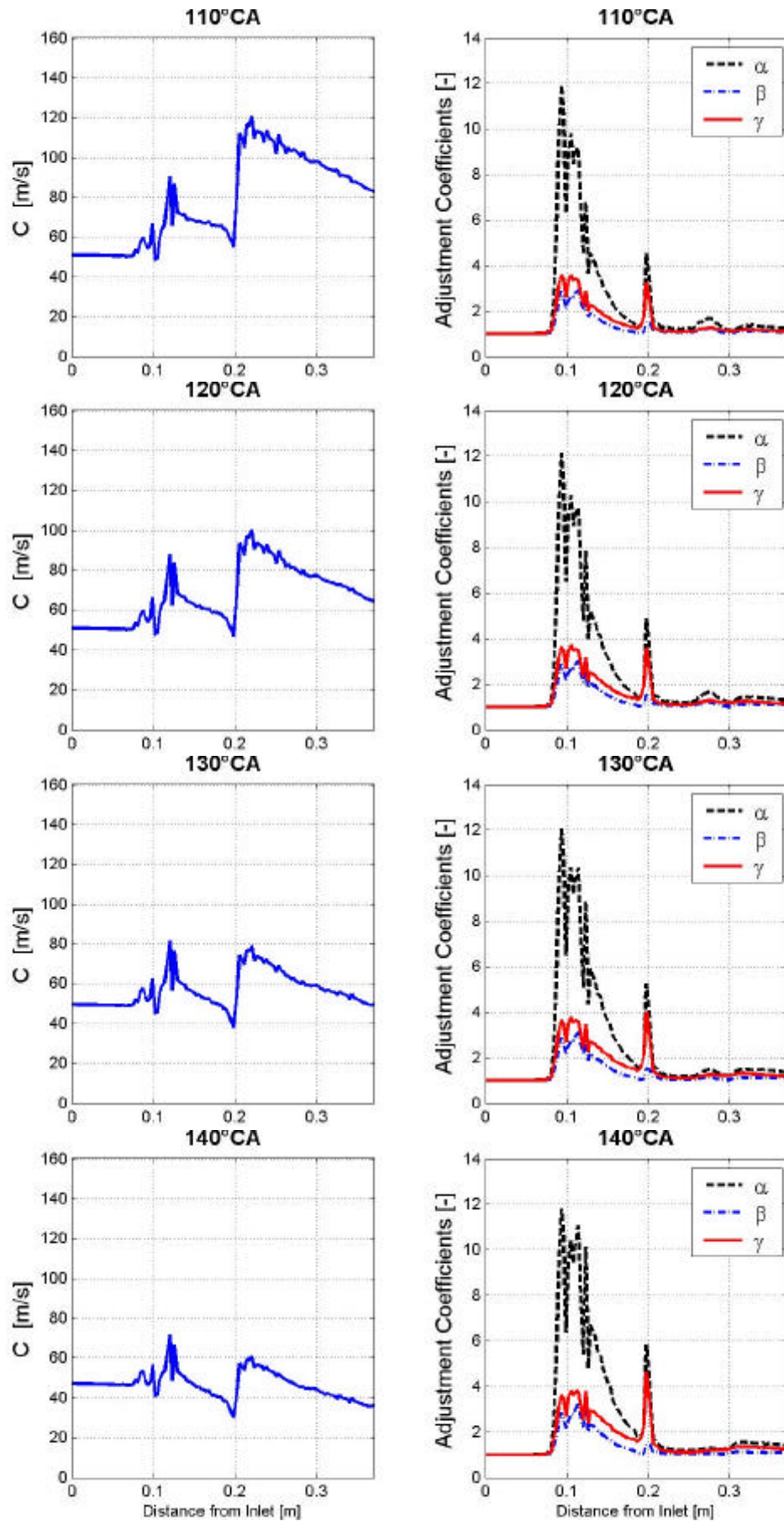


Fig. 7 Averaged axial flow velocity  $C$  and adjustment coefficients variations (continuation)

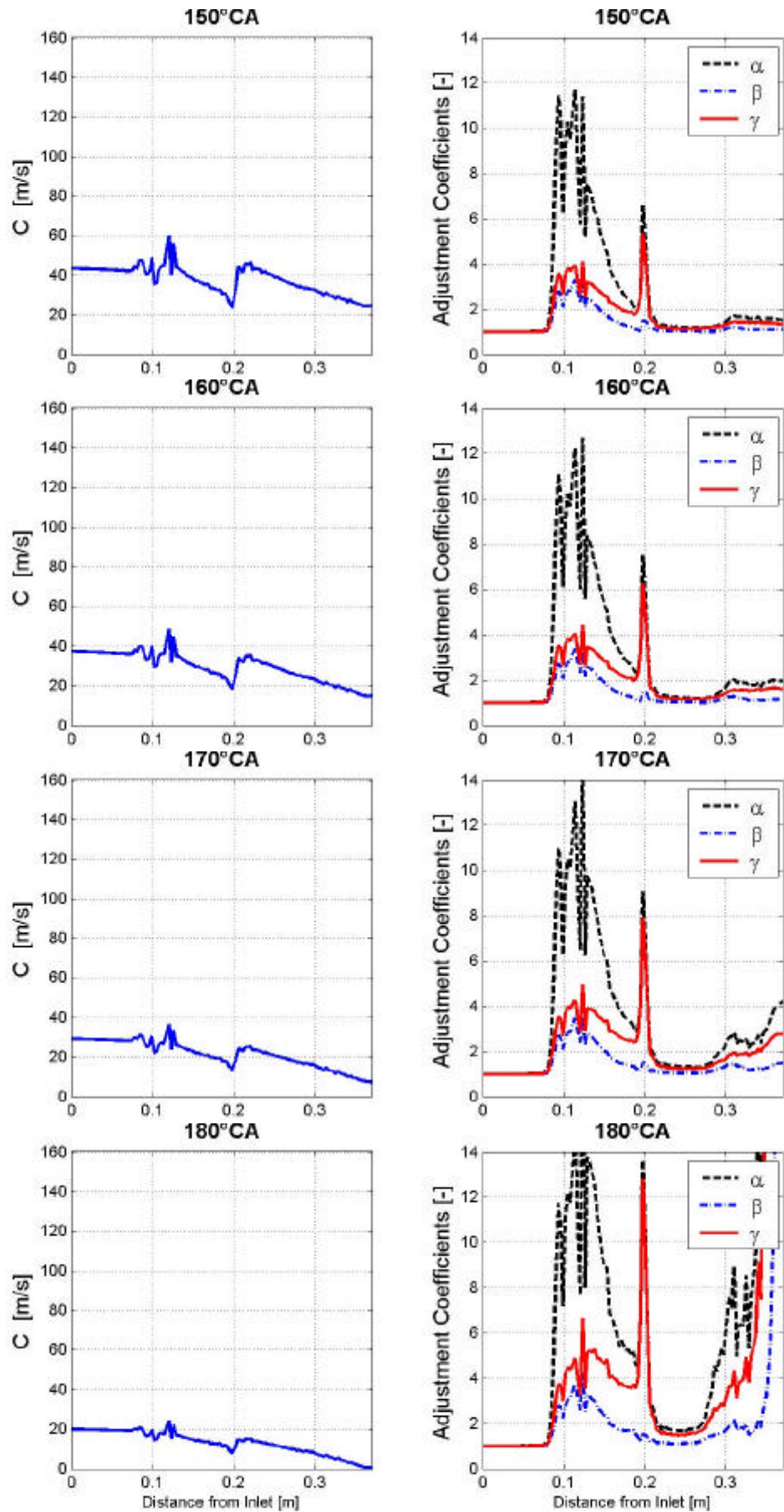
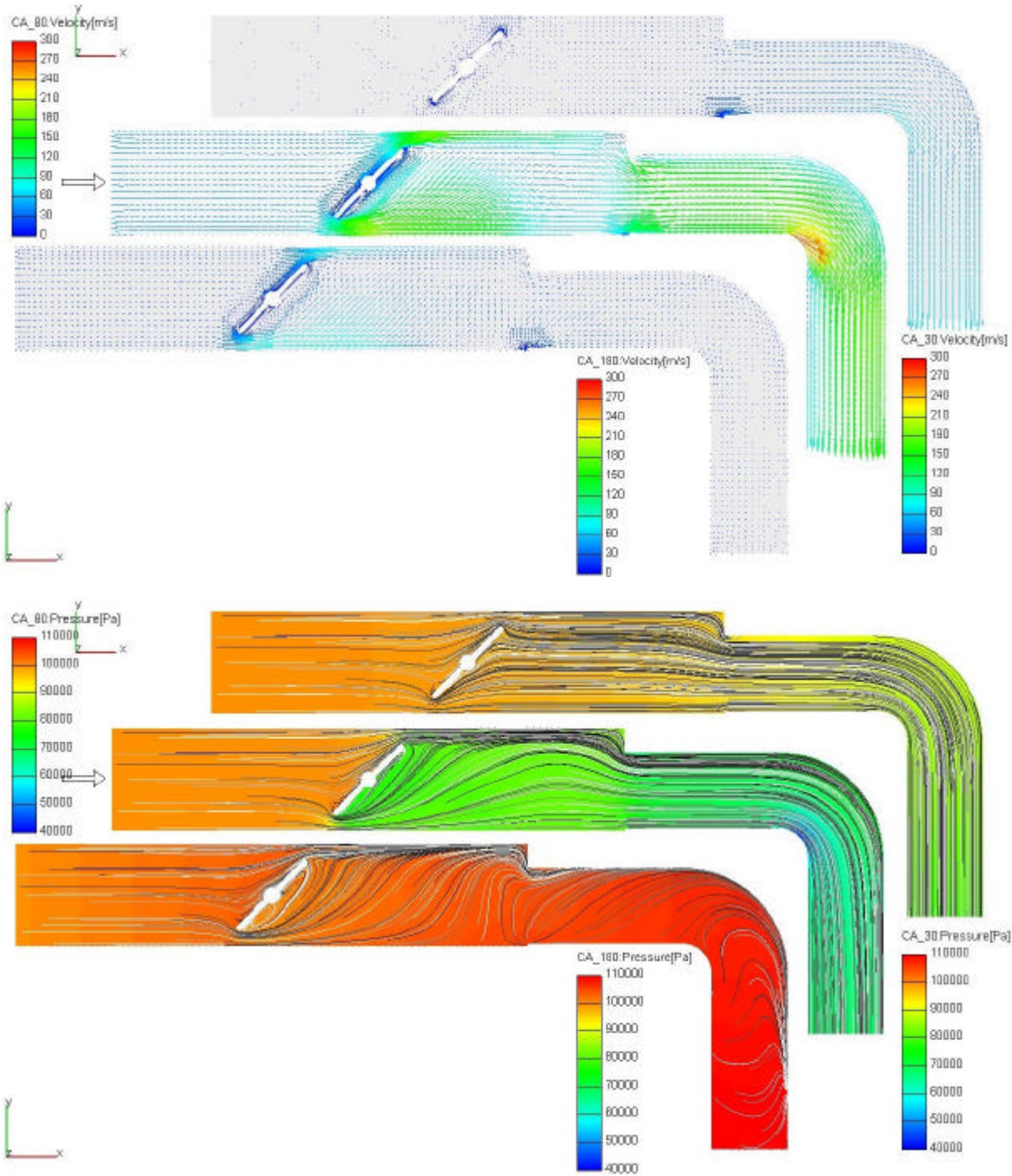


Fig. 7 Averaged axial flow velocity  $C$  and adjustment coefficients variations (continuation)

These results need to be discussed in detail:

- One can observe, that by (very) reduced values of the averaged axial flow velocity  $C$  the adjustment coefficients become bigger (s. Fig. 7 at 10°CA, 170°CA and 180°CA). This behavior is expected because  $C$  appears in the denominator of the adjustment coefficients formula [5], [6], [7] and through there small perturbations of the flow velocity field (s. Fig. 8 at 180°CA) come amplified into effect. On the other hand when  $C$  is small the adjustment coefficients have almost no influence on the integration results of [1]. Consequently one can conclude, that these values of the adjustment coefficients are not significant and for this level of  $C$  no special fitted adjustment coefficients are needed.



**Fig. 8** Flow velocity vectors (up) and absolute pressure with streamlines (down) at 30°CA, 80°CA and 180°CA

- When the flow through throttle port keep on laminar and consequently no recirculation zone behind the throttle are formed (s. Fig. 8 at 30°C<sub>A</sub>), the values of the adjustment coefficient stay at a relative low level (s. Fig 7 at 20°C<sub>A</sub> ... 50°C<sub>A</sub>). In this case one should calculate a first set of adjustment coefficients (for example at 40°C<sub>A</sub>) which can be used as well in the previous case (by (very) reduced values of  $C$ ).
- In the case of high values of  $C$  (s. Fig. 8 at 80°C<sub>A</sub> and Fig.7 at 60°C<sub>A</sub> ... 160°C<sub>A</sub>) a second set of adjustment coefficients is needed. This can be calculated for example with the flow velocity distribution at 100°C<sub>A</sub> and used for the entire interval between 60°C<sub>A</sub> and 160°C<sub>A</sub>.

### Comparison between measurements and quasi-3D simulations

The quasi-3D method is applied to simulate the gas exchange processes of the AVL 520 one-cylinder research engine (s. Fig. 1 and 2), where the adjustment coefficients from Fig. 4 and 5 are used.

The simulation results and the pressure measurements are presented here only in some engine operating points (s. Fig. 9). Along of the intake pipe (apart of the junction between silencer and this pipe, where  $z = 0.14$ ) no other local loss coefficients along of the intake pipe are used in this case.

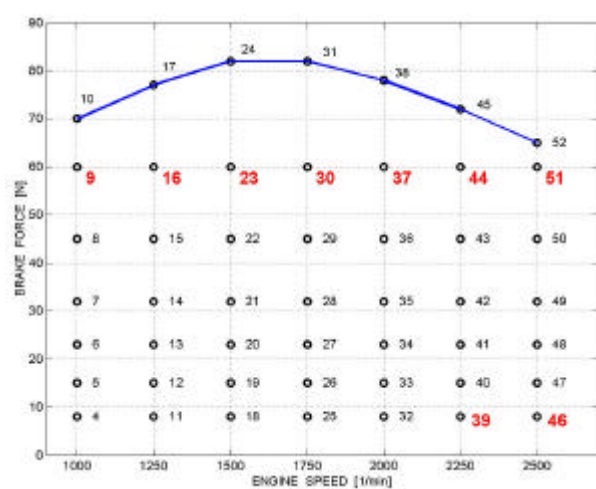


**Fig. 9** Engine operating points map

In the Figures 11 to 19 only the pressure variations comparison at the measuring points 2 and 4 at seven engine speeds and two loads (s. EOPs from Fig. 9) are presented. Presented supplementary are the pressure, flow speed, density, and exhaust gas mass fraction (EGMF) variations as 3D-diagrams, i.e. as isometric illustrations in the distance-crank angle (space-time) plane. In all these 3D-diagrams, the surfaces of the state variables are presented according to the notations from Figure 10.

The comparison between the pressure variations at the measuring points shows quite good agreement between simulations and experiments.

The 3D-diagrams of EGMF for example show the back flows within intake pipe perfectly, and so one can find out when and how intensive these back flows occur. The explanation for the back flows can be found, if one analyzes the 2D- and 3D-diagrams of the intake pressure. The 3D-diagrams for the density show a valley (because of the high exhaust gas temperature) when the back flows occur, while the 3D-diagrams of the flow velocity show negative values. A second back flow could appear when the inlet valve is closing if the cylinder pressure exceeds the intake pipe pressure. The intensity of this second back flow can be captured once again from the 3D-diagrams of EGMF. The 3D-diagrams of the flow velocity and density only confirm these occurrences.

Another example, in case of a MPI ICE it is useful to have the 3D-diagrams of the flow velocity one's disposal. With its help, one can optimize for example the location choice of the gasoline injectors and the intake pipe shape.

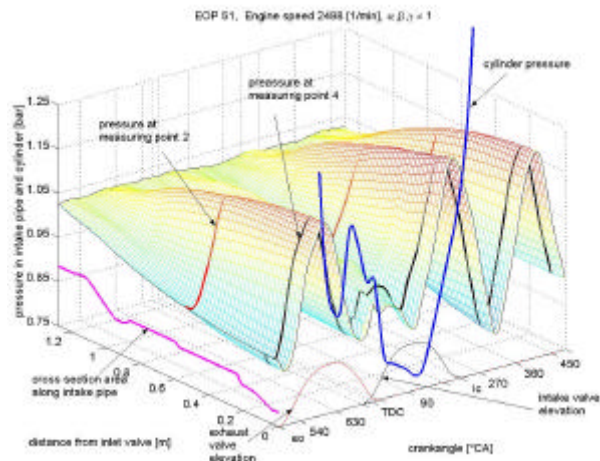


**Fig. 10** 3D-diagram of a state variable in intake pipe as an isomeric illustration in the distance-crank angle (space-time) plane

## CONCLUSIONS

The quasi-3D method allows to take into consideration the real distribution of losses along the pipes (as curvatures, asymmetry of the pipes and channels etc). On the contrary, the classical 1D method requires artificial concentration of the distributed losses in some cross sections, which are treated during the simulation as discontinuity interfaces or boundaries (5), (6). On one hand, the treatment of the boundaries is very time-consuming and causes convergence problems frequently. On the other hand, the simulation results are inaccurate close to the boundaries. This fact becomes more critical because of the complexity of modern manifolds, which requires inserting of a series of boundaries along a pipe.

The quasi-3D method is presented here as a compromise between the 1D and true-3D methods that improves the quality of the 1D-simulation results noticeably, without increasing the cost of computation proportionally.

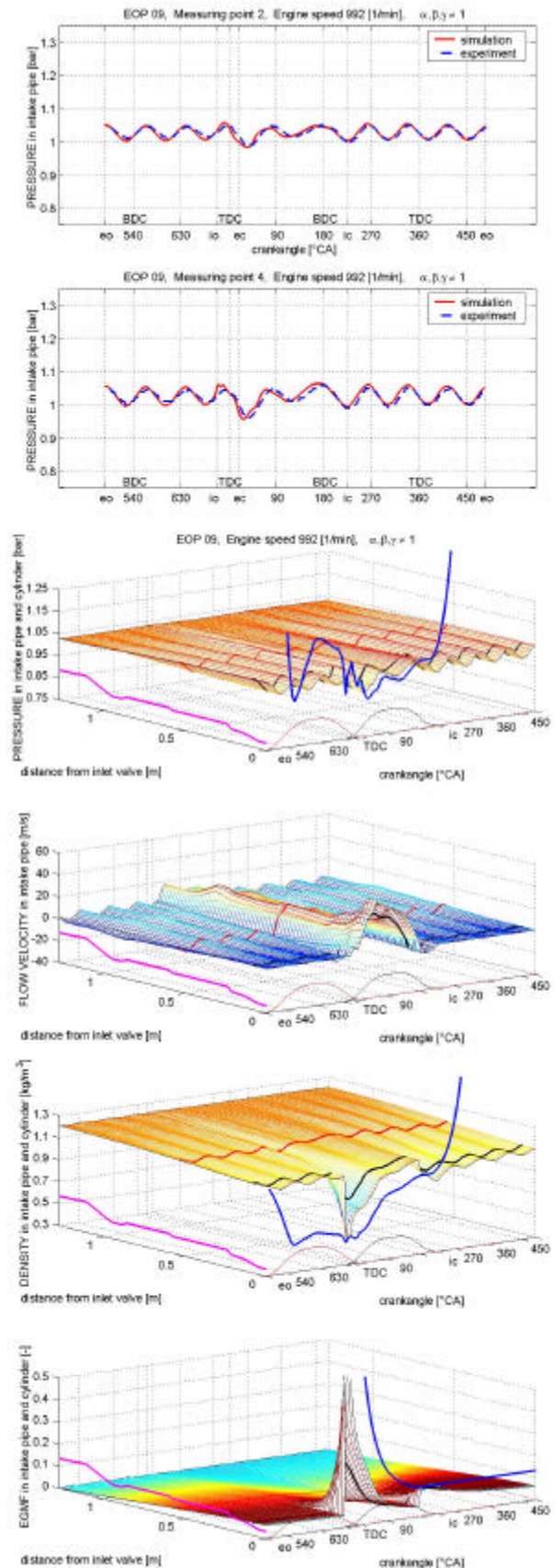


**Fig. 11** Results in EOP 09

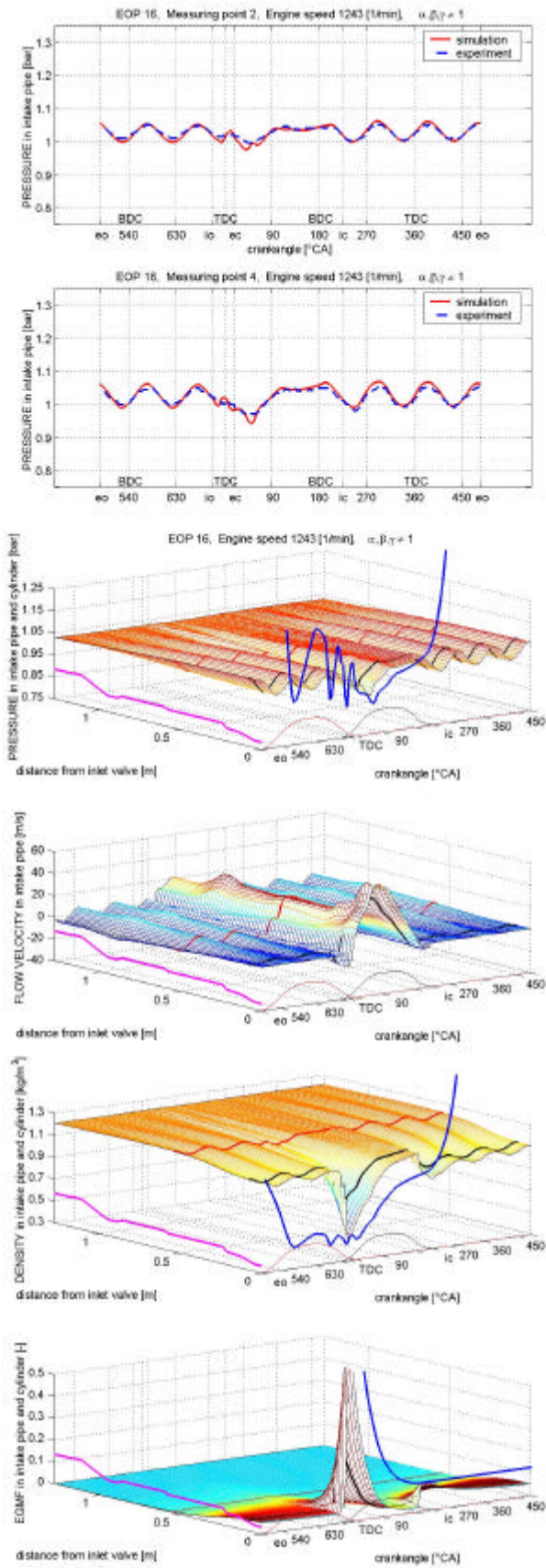


Fig. 12 Results in EOP 16

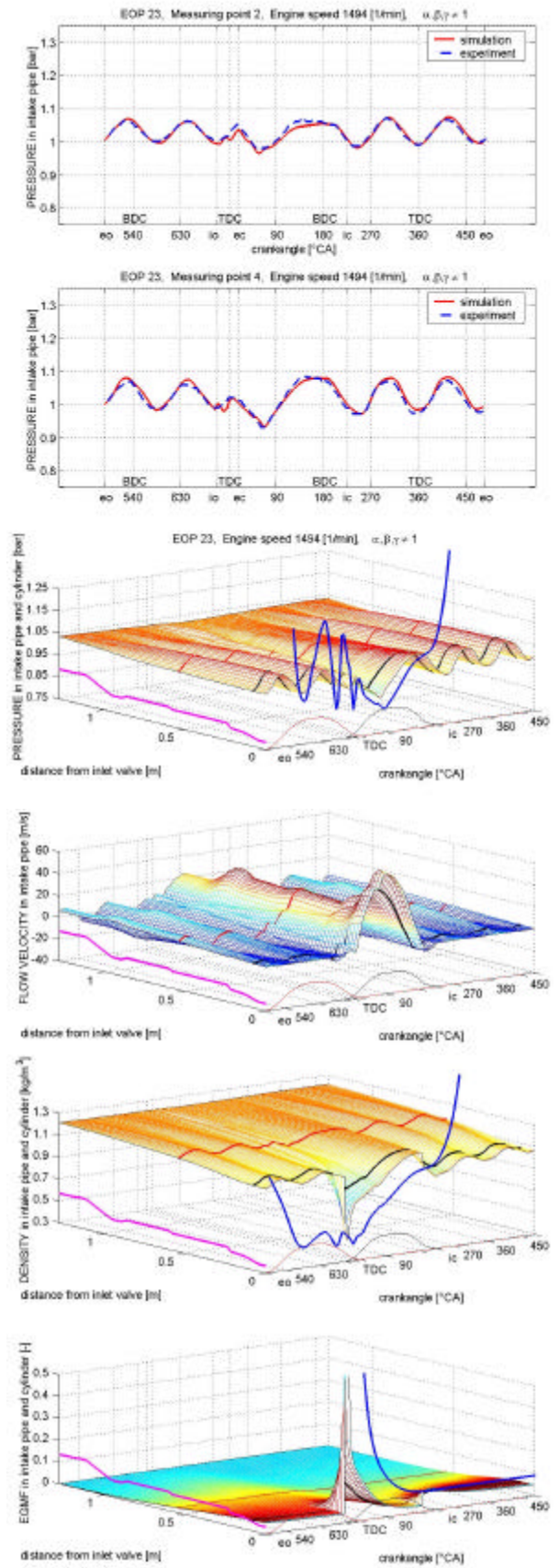


Fig. 13 Results in EOP 23

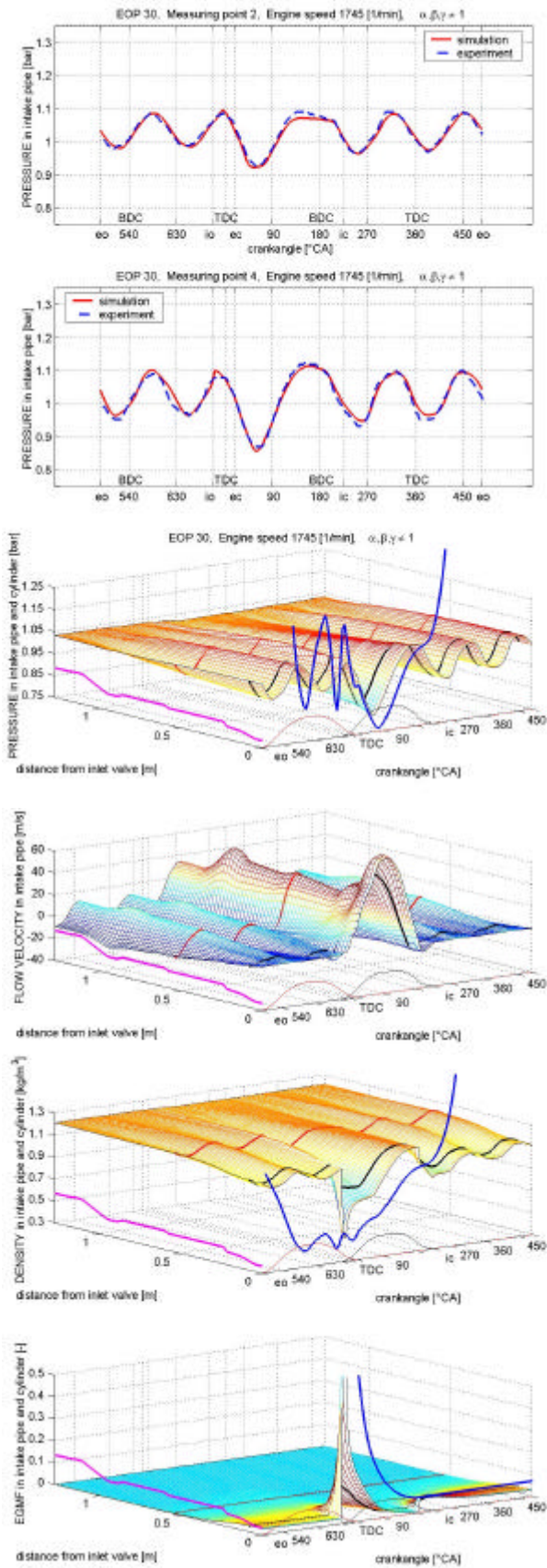


Fig. 14 Results in EOP 30

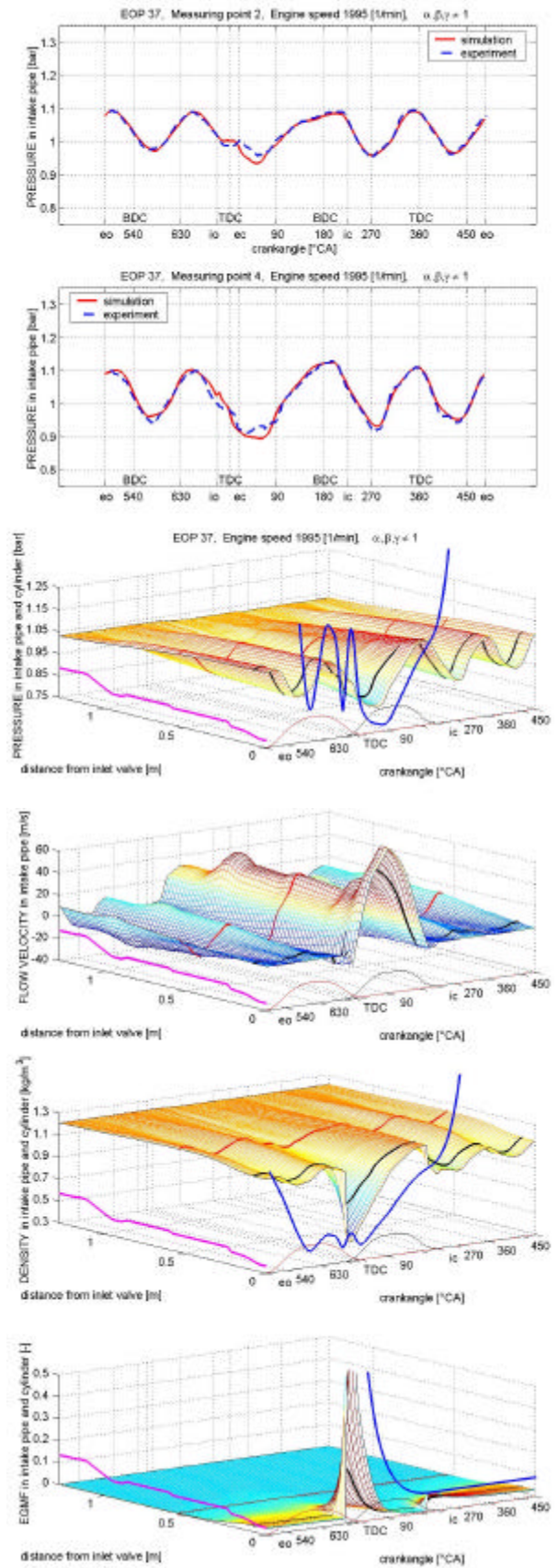


Fig. 15 Results in EOP 37

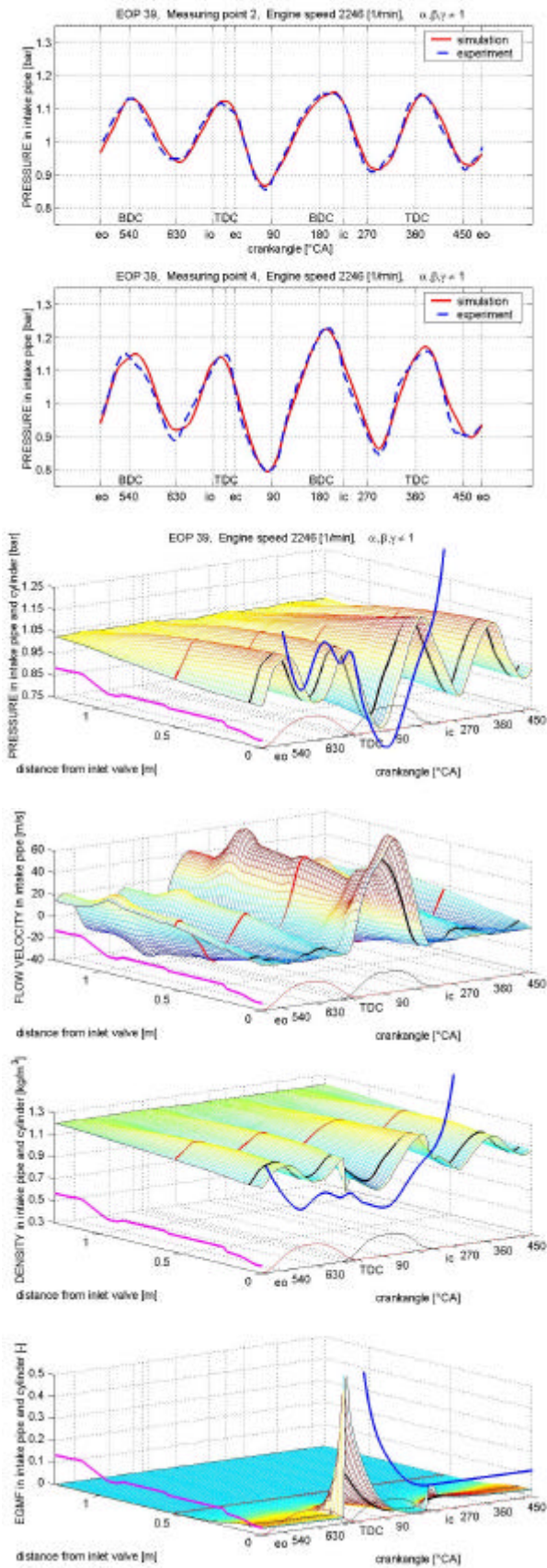


Fig. 16 Results in EOP 39

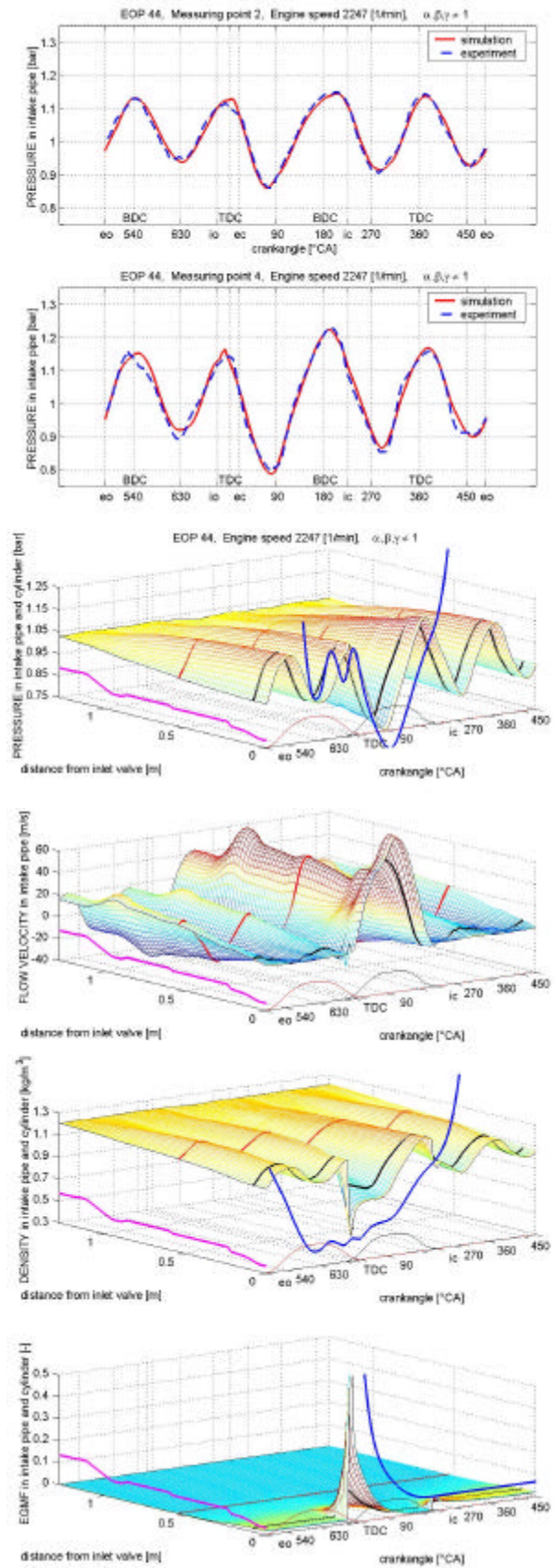


Fig. 17 Results in EOP 44

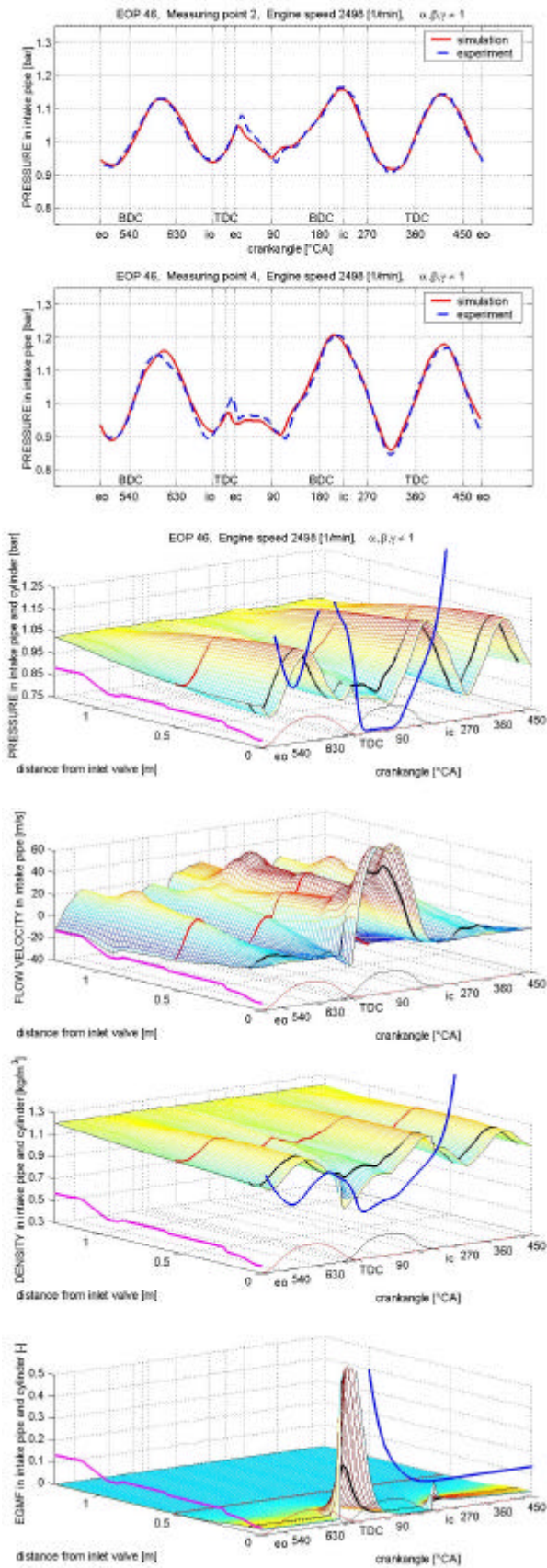


Fig. 18 Results in EOP 46

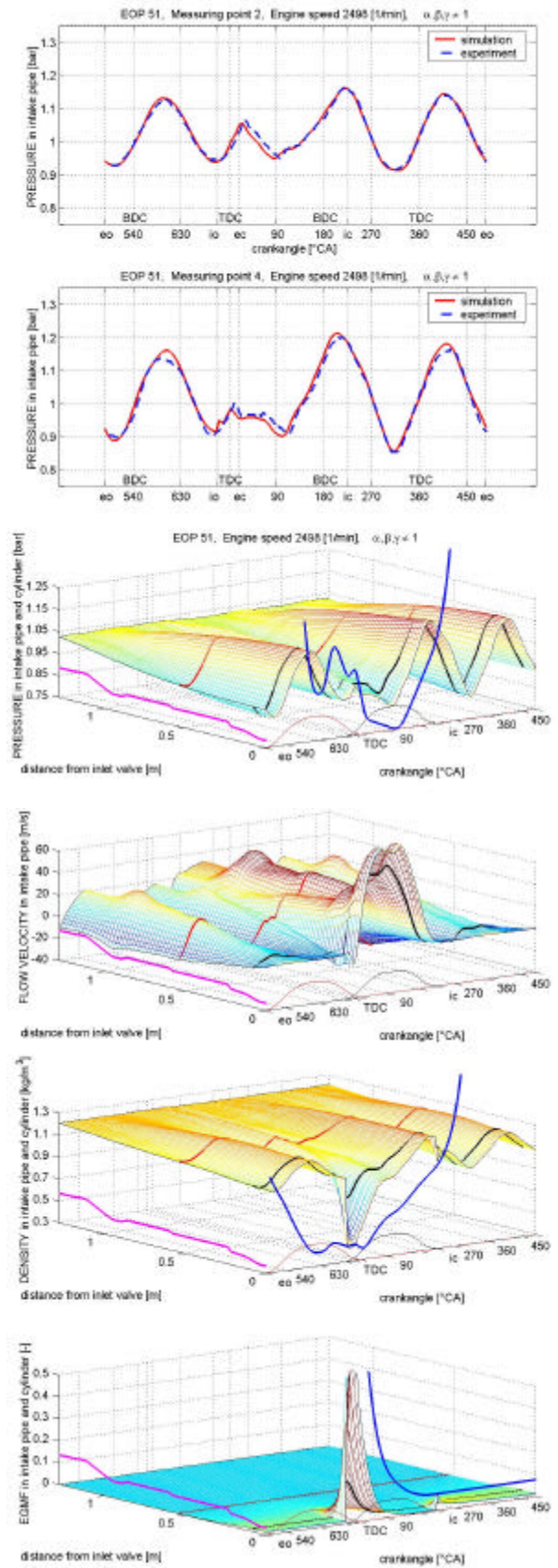


Fig. 19 Results in EOP 51

## REFERENCES

- (1) Boussinesq, I., “Memoire sur l’influence des frottements dans les mouvements réguliers des fluids”, J. de math. pur et appl., nr. 13, p. 377, (French), 1868
- (2) Florea, J., Panaitescu, V., “Mecanica fluidelor”, EDP-Bucuresti, (Romanian), 1979
- (3) Gheorghiu, V., “Higher Accuracy through Combining of quasi-3D (instead of 1D) with true-3D Manifold Flow Models during the Simulation of ICE Gas Exchange Processes”, SAE Paper 2001-01-1913, Orlando, 2001
- (4) Gheorghiu, V., “Quasi-3D Simulation of compressible unsteady flows”, HEFAT, GV1, Victoria Falls, Zambia, 2003
- (5) Seifert, H., “Instationäre Strömungsvorgänge in Rohrleitungen an Verbrennungskraftmaschinen”, Springer Verlag (German), 1962
- (6) Winterbone, D. E., Pearson, R. J., “Design techniques for engine manifolds - Wave action methods for IC engines”, Professional Engineering Publishing, 1999
- (7) Yee, H.-C., “A class of high resolution explicit and implicit shock capturing methods”, Karman Institutes for Fluid Dynamics, Lecture Series 1989-04
- (8) Zierep, J., “Grundzüge der Strömungslehre”, Springer Verlag, (German), 1997